Polymer Engineering & Science

WILEY | spe INSPIRING PLASTICS PROFESSIONALS

RESEARCH ARTICLE OPEN ACCESS

Rheological Characterization of a Low-Concentration Water-Based Collagen Dispersion Under Extensional, Shear, and Oscillatory Deformation

Fadi Alzarzouri[1] | Xiaohe Xu[2] | Manfred Wilhelm[2] | Jan Skočilas[1]

[1]Faculty of Mechanical Engineering, Czech Technical University in Prague, Prague, Czech Republic | [2]Institute of Chemical Technology and Polymer Chemistry, Karlsruhe Institute of Technology, Karlsruhe, Germany

Correspondence: Fadi Alzarzouri (fadi.alzarzouri@fs.cvut.cz)

Received: 30 April 2026 | **Revised:** 20 June 2026 | **Accepted:** 22 June 2026

Keywords: capillary rheometer | collagen | extensional viscosity | FT-rheology | SAOS and LAOS | viscoelastic behavior

ABSTRACT

This study presents an investigation of the extensional, shear, and oscillatory rheological behavior of a 3 wt% native bovine collagen dispersion using capillary rheometer and oscillatory shear testing. Extensional viscosity was determined from the entrance pressure drop using Cogswell's analysis. The entrance pressure drop was obtained through both Bagley extrapolation and orifice die methods. The close agreement between Bagley and orifice die results confirms the reliability of the entrance pressure measurements and indicates that the fabricated orifice die can be used for direct entrance pressure drop determination within the investigated range. The collagen dispersion exhibited pronounced shear thinning and extensional thinning behavior. The apparent shear viscosity (η_{app}) decreased from approximately $\eta_{app} = 250$ Pa·s to $\eta_{app} = 6.3$ Pa·s while the extensional viscosity (η_E) decreased from approximately $\eta_E = 1.6 \times 10^6$ Pa·s to $\eta_E = 3.4 \times 10^4$ Pa·s over the investigated deformation rate range. Small and large amplitude oscillatory shear (SAOS and LAOS) measurements showed solid-like viscoelastic behavior in the linear regime and nonlinear viscoelastic behavior at large strain amplitudes. Fourier transform (FT) rheology results showed a progressive increase in higher harmonic contributions with increasing strain amplitude. Results are relevant for the design and optimization of collagen-based food, biomedical, and extrusion processes.

1 | Introduction

Extensional viscosity is a critical rheological parameter for characterizing the non-shear deformation behavior of food materials [1, 2]. Extensional viscosity plays an essential role in process design, product development, and quality assurance, as well as in the modeling and optimization of numerous food processing operations [1, 2]. Extensional flow becomes relevant in processes involving stretching or elongation, such as extrusion, contraction flows, fiber spinning, and blow molding [3]. In food systems, similar deformation mechanisms occur frequently during protein extrusion [4], dough kneading [5], and cheese stretching [6]. Hence, evaluation of extensional viscosity is essential for optimizing processing conditions and ensuring desirable product characteristics.

Various experimental techniques, such as Sentmanat extensional rheometer (SER) [7], extensional viscosity fixture (EVF) [8–11], filament-stretching extensional rheometers (FiSER) [11, 12], and capillary break-up extensional rheometers (CaBER) [13, 14], have been developed to evaluate the extensional flow properties of materials. Most of these methods are primarily suited for highly viscous materials such as polymer melts and doughs that can be formed into stable filaments or sheets. However, they are unsuitable for low viscosity fluids like protein solutions, which cannot maintain a well-defined shape due to their mobile nature [3, 15]. In contrast, the entrance pressure drop method offers a practical approach for determining extensional viscosity in both low and high viscosity fluids using a conventional capillary rheometer [16]. In this method, the contraction flow at the capillary

Highlights

- Extensional, shear, and oscillatory rheology of collagen.
- Pronounced shear and extensional thinning behavior of collagen.
- Close agreement in entrance pressure from Bagley correction and orifice die.
- SAOS and LAOS reveal linear and nonlinear viscoelastic responses.
- Quantitative data for modeling and prediction of collagen extrusion behavior.

entrance generates an extensional flow field, from which extensional viscosity can be derived using the method proposed by Cogswell [17, 18]. This method relates the measured entrance pressure drop to the corresponding apparent extensional stress and apparent extensional rate to calculate the extensional viscosity [17, 18]. The Cogswell approach has previously been reported as a practical method for estimating extensional viscosity from entrance pressure drop in viscoelastic food materials [4].

The entrance pressure drop can be obtained either through Bagley correction or by using an orifice die, defined by its very small length-to-diameter (L/D) ratio [16, 19–24]. The Bagley method involves plotting the measured capillary pressure drop as a function of the length-to-diameter ratio of the capillary dies at various apparent shear rates [16, 20]. Extrapolation of the measured pressure data to zero length of capillary provides the entrance pressure drop [20]. This procedure typically requires measurements using at least two capillaries of the same diameter but different lengths, while using three capillaries is preferable for improving accuracy [20]. As a simpler alternative, the orifice die method directly measures entrance pressure drop using a very short die, eliminating the need for extrapolation and simplifying the experimental procedure.

Reliable estimation of the entrance pressure drop using the Bagley approach is highly sensitive to both the selection of capillary L/D ratios and the accuracy of the extrapolation procedure [16, 20]. In contrast, measurements obtained using an orifice die depend critically on the die geometry, particularly the L/D ratio, entrance angle, and outlet design, which must be configured to prevent the extrudate polymer from adhering to the downstream die walls. Adhesion or sticking of the polymer at the orifice die exit can introduce additional flow deformation, leading to an overestimation of the entrance pressure drop [21–24]. Padmanabhan and Macosko [16] reported that for low-density polyethylene (LDPE), the entrance pressure drops obtained via Bagley extrapolation were higher than those measured directly with an orifice die. They attributed this result to uncertainty associated with the extrapolation process. Sunder and Goettfert [20] emphasized that obtaining reliable Bagley corrections requires an appropriate selection of capillary lengths that differ sufficiently to prevent error accumulation. They recommended using dies with L/D ratios of approximately 5, 10, and 20 to minimize the accumulation of small measurement errors. Kelly et al. [21] investigated the flow behavior of linear low-density polyethylene (LLDPE) using a twin-bore capillary rheometer equipped with six orifice dies of 1 mm diameter and L/D ratios ranging from 0.1 to 1. They found that for dies with $L/D \leq 0.5$, the L/D ratio had little influence on the measured entrance pressure drop. Kim and Dealy [22] found that an orifice die with an entrance angle greater than 90° and a sufficiently widened exit section yields reliable measurements. Under these conditions, the entrance pressure drop measured directly with the orifice die agreed closely with the values obtained from Bagley extrapolation for both LLDPE and linear metallocene polyethylene (LmPE). Zatloukal and Musil [23] demonstrated through combined theoretical and experimental analysis on LDPE that melt contact with the downstream region of a conventional orifice die leads to an overestimation of the entrance pressure drop. To overcome this issue, they developed and tested a modified orifice die with an open exit section, which effectively eliminated the artificial pressure increase and produced more accurate and reproducible entrance pressure measurements. Aho and Syrjala [24] compared entrance pressure drops obtained from Bagley extrapolation and an orifice die for LDPE and polystyrene (PS) melts. They found that the orifice die method yielded higher entrance pressure values, primarily due to melt adhesion at the die exit.

Collagen and collagen-based materials are widely used in food, biopharmaceutical, and cosmetic industries [25]. Applications include biological dressings, tissue scaffolds, sausage casings, and other collagen-derived food products [25, 26]. The global collagen market reached approximately 4.7 billion USD in 2020, with the food and beverage (~32%) and health management (~48%) sectors accounting for nearly 80% of total consumption [27]. This market is projected to grow to about 7 billion USD by 2027 (ca. 6% per year) [27]. The increasing industrial relevance of collagen highlights the need for a fundamental understanding of its flow behavior for designing and optimizing processes such as extrusion, pumping, and kneading [28]. In contrast, previous rheological studies of water-based native collagen using capillary rheometers have focused mainly on shear viscosity measurements [28–31], whereas extensional viscosity measurements using capillary rheometers have not yet been reported for native collagen dispersions. Consequently, the extensional rheological behavior of native collagen dispersions obtained from capillary rheometers remains largely unexplored.

On the other hand, several studies have investigated the viscoelastic behavior of collagen-based materials using small and large amplitude oscillatory shear (SAOS and LAOS) testing [28, 32–39]. Štípek et al. [39] performed SAOS measurements on water-based native collagen dispersions with concentrations ranging from 1.5 to 7.6 wt% and reported that both storage and loss moduli increased with increasing collagen concentration. However, their LAOS measurements were limited to a collagen concentration of 6 wt%. In contrast, most oscillatory shear studies have focused on acid- or pepsin-solubilized collagen gels rather than water-based native collagen dispersions [32–38]. Therefore, the nonlinear viscoelastic behavior of water-based native collagen dispersions, especially at low concentrations, remains poorly characterized and quantified and requires further investigation.

This study investigates the extensional and shear flow behavior of a low-concentration (3 wt%) water-based native collagen

dispersion using a capillary rheometer. The extensional viscosity is determined from the entrance pressure drop using the Cogswell method. The entrance pressure drop is obtained using both the Bagley correction and the orifice die techniques. In addition, small and large amplitude oscillatory shear (SAOS and LAOS) tests were performed to characterize both the linear and nonlinear viscoelastic properties of the collagen dispersion. Collagen gels used in co-extruded food casing applications typically contain 3–6 wt% collagen, placing the concentration of 3 wt% at the lower bound of industrial relevance [26]. Therefore, the concentration selected in this study is relevant from both industrial and scientific perspectives. By combining shear, extensional, and oscillatory rheological measurements at this concentration, this study provides a comprehensive rheological characterization of water-based native collagen dispersions and fills a gap in the quantitative characterization of low-concentration collagen dispersions under shear, extensional, and oscillatory deformation. To the best of our knowledge, extensional rheology obtained from capillary entrance pressure analysis and nonlinear viscoelastic characterization using LAOS has not previously been reported for a low-concentration water-based native collagen dispersion. The results provide relevant data for optimizing collagen-based processing operations.

2 | Materials and Methods

2.1 | Materials

The material investigated in this study was an aqueous dispersion of native bovine collagen Type I obtained from bovine skin. The collagen was supplied by Devro Ltd. (Jilemnice, Czech Republic), a company specializing in producing collagen casings for the food industry. The dispersion contained 3 wt% collagen, and no chemical additives were used. Before the experiments, the samples were stored in a refrigerator at 10°C ± 1°C in evacuated bags to prevent chemical reactions, specifically oxidation, humidification, and degradation.

2.2 | Capillary Rheometer and Experimental Setup

Rheological measurements of the collagen dispersion were performed using a Goettfert Rheograph (RG 50, with 50 kN maximum force) capillary rheometer operated at the Institute for Chemical Technology and Polymer Chemistry (ITCP), Karlsruhe Institute of Technology (KIT), Germany. The collagen dispersion was loaded into the rheometer barrel and compressed by the piston at a controlled speed to force the material through the capillary die. Care was taken during loading to minimize trapped air and ensure uniform filling of the barrel. Based on the recordings from the pressure transducer (0–200 bar, Goettfert, Germany) the software of the capillary rheometer provided the total pressure drop during each measurement. The flow rate is obtained from the displacement of the piston and its area. Figure 1 shows a schematic of the capillary rheometer setup used for the measurements. As illustrated in Figure 1, the total pressure drop associated with flow through a capillary die of length L and diameter D can be expressed as:

$$\Delta P_{\text{Total}} = \Delta P_{\text{Cap}} + \Delta P_{\text{Ent}} \quad (1)$$

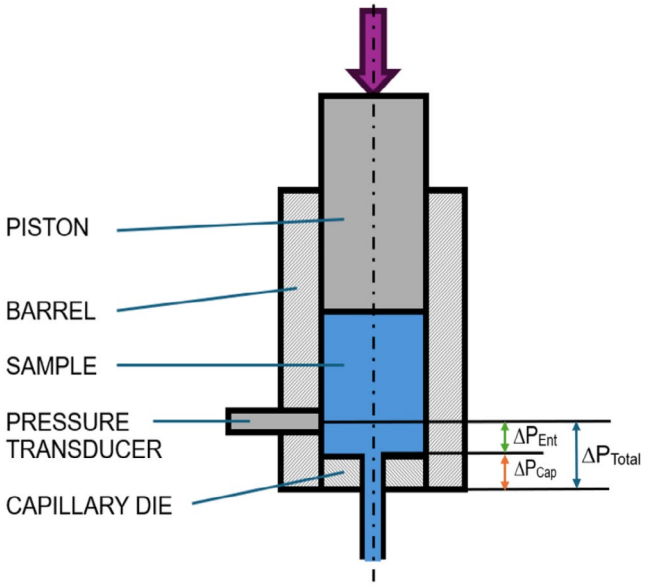

FIGURE 1 | Schematic of the capillary rheometer showing the piston, barrel, capillary die, and the pressure drop components: Total pressure drop ΔP_{Total}, pressure drop over the capillary die length ΔP_{Cap}, and entrance pressure drop ΔP_{Ent}.

where ΔP_{Total} represents the total pressure drop, ΔP_{Cap} corresponds to the pressure drop due to shear flow over the capillary length, and ΔP_{Ent} represents the entrance pressure drop associated with extensional flow at the die entry.

The entrance pressure drop was determined using two approaches: the Bagley correction method and the orifice die technique. For the Bagley correction, three circular capillary dies with a constant diameter ($D = 2$ mm) and lengths of 10, 20, and 30 mm were used. These geometries correspond to L/D ratios of 5, 10, and 15, respectively. The measured total pressure drops for each geometry were plotted as a function of the corresponding L/D ratio. Linear extrapolation of these data to $L = 0$ yielded the intersections, which represent the entrance pressure drops.

For the orifice die method, a short circular die with $L = 0.8$ mm and $D = 2$ mm ($L/D = 0.4$) and an entrance angle of 180° was designed and manufactured at ITCP, Karlsruhe Institute of Technology (KIT), Germany. The die incorporates a wide-open downstream section that could prevent contact between the collagen sample and the die wall, thereby eliminating artificial pressure increases. This design could provide a more accurate determination of the entrance pressure drop. The orifice die is also equipped with four symmetrically arranged holes that enable mechanical attachment to the rheometer barrel through a screw-based connection system. A photograph of the fabricated orifice die is shown in Figure 2.

A comparative analysis was performed to assess the agreement between entrance pressure values obtained using the Bagley method and those derived from orifice die measurements. This comparison evaluates the consistency of both approaches in characterizing the extensional flow behavior of collagen. All measurements were conducted at room temperature (25°C). Apparent shear rates of 10, 100, 300, 500, and 1000 s^{-1} were

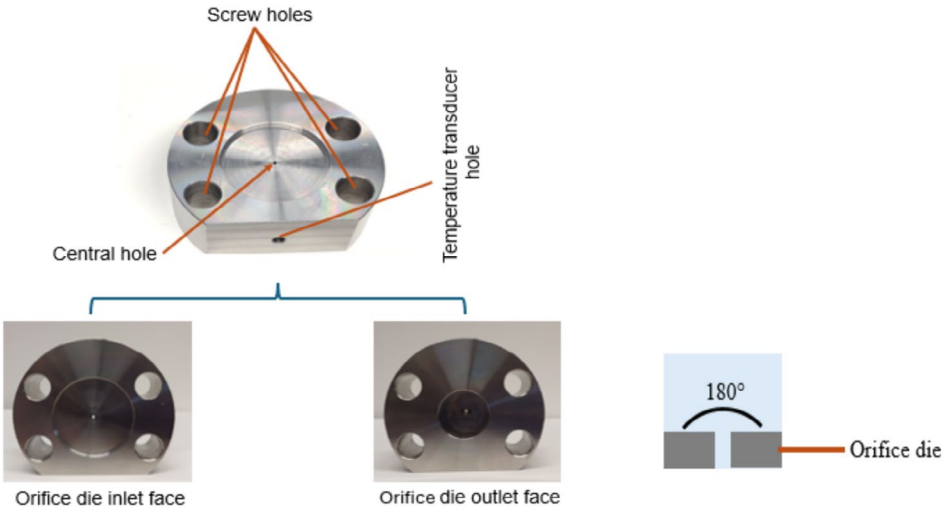

FIGURE 2 | Photograph of the orifice die ($L = 0.8$ mm, $D = 2$ mm, $L/D = 0.4$, entrance angle = 180°) designed and manufactured at ITCP, Karlsruhe Institute of Technology (KIT), Germany.

applied. Each measurement was repeated at least three times, and the average values were used for data analysis.

2.3 | Cogswell Model and Calculation Procedure

The extensional viscosity was calculated using the Cogswell model based on the measured entrance pressure drop. This model assumes that the material exhibits extensional flow at the die entrance. The following relations were applied [18]:

$$\sigma_E = \frac{3\,(n+1)\,\Delta P_{\mathrm{Ent}}}{8} \tag{2}$$

$$\dot{\varepsilon}_E = \frac{4\,\eta_{\mathrm{app}}\dot{\gamma}_{\mathrm{app}}^2}{3(n+1)\,\Delta P_{\mathrm{Ent}}} \tag{3}$$

$$\eta_E = \frac{\sigma_E}{\dot{\varepsilon}_E} = \frac{9\,(n+1)^2\Delta P_{\mathrm{Ent}}^2}{32\,\eta_{\mathrm{app}}\dot{\gamma}_{\mathrm{app}}^2} \tag{4}$$

where η_E is the apparent extensional viscosity, σ_E is the apparent extensional stress, $\dot{\varepsilon}_E$ is the apparent extensional rate, ΔP_{Ent} is the entrance pressure drop.

The shear flow behavior of collagen was determined using the Ostwald-de Waele (power law) model:

$$\tau_{\mathrm{corr}} = K\,\dot{\gamma}_{\mathrm{app}}^{n} \tag{5}$$

where K is the consistency index. $\dot{\gamma}_{\mathrm{app}}$, τ_{corr}, η_{app}, and n can be determined from [40, 41]:

$$\dot{\gamma}_{\mathrm{app}} = \frac{4\mathrm{Q}}{\pi R^3} \tag{6}$$

$$\tau_{\mathrm{corr}} = \frac{\Delta P_{\mathrm{Cap}}\cdot R}{2L} = \frac{\left(\Delta P_{\mathrm{Total}} - \Delta P_{\mathrm{Ent}}\right)\cdot R}{2L} \tag{7}$$

$$\eta_{\mathrm{app}} = \frac{\tau_{\mathrm{corr}}}{\dot{\gamma}_{\mathrm{app}}} \tag{8}$$

$$n = \frac{d\left(\log\,\tau_{\mathrm{corr}}\right)}{d\left(\log\,\dot{\gamma}_{\mathrm{app}}\right)} \tag{9}$$

where Q is the volumetric flow rate and R is the radius of the die. $\dot{\gamma}_{\mathrm{app}}$ is the apparent shear rate, τ_{corr} is the corrected shear stress, η_{app} is the apparent shear viscosity, and n is the exponent of the power law model describing flow behavior.

As shear flow is often modeled using a power law relation, the extensional flow can also be represented using a power law formulation for extensional flow [42]. The experimental datasets of the apparent extensional stress as a function of the apparent extensional rate will be described as follows:

$$\sigma_E = K_e\,\dot{\varepsilon}_E^{\,n_e} \tag{10}$$

where K_e and n_e define the power law model parameters for extensional flow.

The corrected shear rate ($\dot{\gamma}_{\mathrm{corr}}$) was determined from the Rabinowitsch–Weissenberg correction as [43]:

$$\dot{\gamma}_{\mathrm{corr}} = \frac{4Q}{\pi R^3}\,\frac{3n+1}{4n} \tag{11}$$

It is important to note that the derivation of the Cogswell model for calculating extensional viscosity was originally developed without applying the Rabinowitsch–Weissenberg correction to maintain analytical simplicity [17]. According to Cogswell, introducing this correction would greatly increase the mathematical complexity [17]. As a result, the Cogswell model is expressed in terms of the apparent shear viscosity [17]. In the present work, the Rabinowitsch–Weissenberg correction is therefore not applied within the Cogswell framework, as the model is formulated using the apparent shear viscosity, which was calculated as described in Equation (7). However, this correction is applied to determine the true shear viscosity (η_{true}), as presented in Equation (12) below, for comparison with the apparent shear viscosity.

$$\eta_{\mathrm{true}} = \frac{\tau_{\mathrm{corr}}}{\dot{\gamma}_{\mathrm{corr}}} \tag{12}$$

Zatloukal et al. [40] introduced the concept of entrance viscosity to provide a more general and precise physical description of the viscosity behavior across a wide range of apparent shear rates. Entrance viscosity is defined as [40]:

$$\eta_{Ent} = \frac{\Delta P_{Ent}}{\dot{\gamma}_{app}} \tag{13}$$

The orifice die method assumes that the capillary pressure drop is negligible and therefore the measured total pressure drop is equal to the entrance pressure drop.

$$\Delta P_{Total} = \Delta P_{Ent} \tag{14}$$

2.4 | Oscillatory Shear Testing

Small amplitude oscillatory shear (SAOS) and large amplitude oscillatory shear (LAOS) tests were performed using a strain-controlled rheometer (ARES G2, TA Instruments) equipped with a 25 mm cross-hatched parallel plate geometry and a 1 mm gap. The temperature was maintained at 25°C ± 0.1°C using a Peltier-controlled system. A solvent trap was used throughout the tests to minimize moisture loss and ensure temperature stability of the collagen samples. SAOS testing was performed to evaluate the linear viscoelastic (LVE) behavior of the collagen dispersion. A dynamic strain sweep was first conducted at a constant frequency of $\omega = 1$ Hz with strain amplitudes ranging from $\gamma_0 = 0.01\%$ to 995%. The applied strain amplitude range covers both the linear viscoelastic (LVE) and nonlinear viscoelastic regimes, allowing identification of the LVE regime. Based on these results, a dynamic frequency sweep was then performed within the LVE region at a fixed strain amplitude of $\gamma_0 = 1.0\%$ over a frequency range of $\omega = 0.1$–100 Hz. To assess the nonlinear viscoelastic behavior, LAOS testing was conducted at a constant frequency of $\omega = 1$ Hz with strain amplitudes ranging from $\gamma_0 = 2.7\%$ to 995%. The nonlinear material response was analyzed using Lissajous–Bowditch plots to visualize the stress–strain behavior during the oscillation cycle, and Fourier transform (FT) rheology to provide a quantitative characterization of nonlinear viscoelasticity. All SAOS measurements represent the mean of two independent replicates. For LAOS measurements, a single test was conducted and representative plots of Lissajous–Bowditch and FT-rheology are reported.

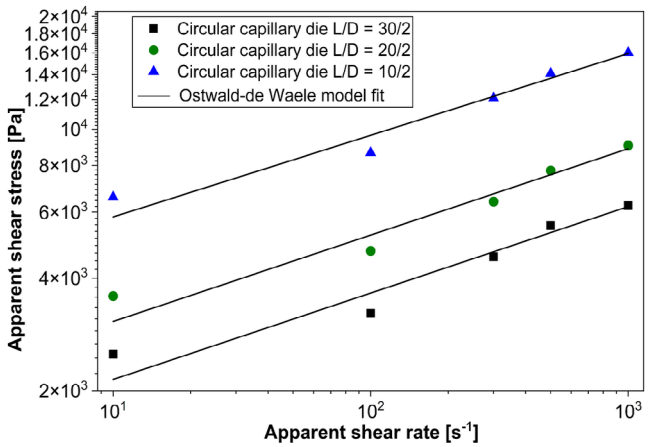

FIGURE 3 | Apparent shear stress as a function of apparent shear rate for collagen 3 wt%.

3 | Results and Discussion

3.1 | Shear Flow Behavior

Figure 3 shows the relationship between apparent shear stress and apparent shear rate for the 3 wt% collagen dispersion measured using three dies with different L/D ratios. The apparent shear stress here refers to values calculated directly from the total pressure drop without subtracting the entrance pressure via the Bagley method. All datasets are described by the Ostwald-de Waele (power law) model. Table 1 presents Ostwald-de Waele model parameters derived from the apparent shear stress versus apparent shear rate data without applying any corrections. Table 2 shows Ostwald-de Waele model parameters after applying only the Bagley correction and after applying both Bagley and Rabinowitsch–Weissenberg corrections. The flow behavior index n obtained after applying only the Bagley correction was used in the Cogswell method to estimate extensional viscosity, since the Cogswell model was originally derived using uncorrected shear rates to maintain analytical simplicity, as noted in the Methods section. The parameters obtained after applying both the Bagley and Rabinowitsch–Weissenberg corrections were used to compute the true shear viscosity of the collagen dispersion.

Figure 4 presents both the apparent and true shear viscosity as functions of shear rate for the $L/D = 30/2$ capillary die. In both cases, viscosity decreases with increasing shear rate, indicating

TABLE 2 | Ostwald-de Waele model parameters after Bagley correction (used for extensional viscosity calculation) and after Bagley and Rabinowitsch–Weissenberg corrections (used for true shear viscosity calculation).

Circular capillary die $L/D = 30/2$			Circular capillary die $L/D = 30/2$		
Parameters after Bagley correction			Parameters after Bagley and Rabinowitsch–Weissenberg corrections		
K (Pa·s^n)	n (–)	R^2	K (Pa·s^n)	n (–)	R^2
143.43	0.32	0.87	125.15	0.32	0.87

TABLE 1 | Ostwald-de Waele model parameters from apparent shear stress versus apparent shear rate (uncorrected data).

Circular capillary die			Circular capillary die			Circular capillary die		
$L/D = 30/2$			$L/D = 20/2$			$L/D = 10/2$		
K (Pa·s^n)	n (–)	R^2	K (Pa·s^n)	n (–)	R^2	K (Pa·s^n)	n (–)	R^2
1258.19	0.23	0.96	1798.93	0.23	0.97	3525.02	0.22	0.97

pronounced shear thinning behavior. As the shear rate increases, the forces binding collagen molecules are progressively disrupted. This allows the molecules to move more freely past one another, resulting in a pronounced decrease in viscosity [44]. The apparent shear viscosity remains higher than the true viscosity across the entire range. After applying the Bagley and Rabinowitsch–Weissenberg corrections, the viscosity curve shifts downward. This highlights the importance of applying these corrections to obtain an accurate representation of the shear viscosity.

The flow behavior indices ($n < 1$) presented in Tables 1 and 2 confirm the shear thinning behavior of the collagen dispersion. The decrease in the consistency index (K) and the slight increase in the flow behavior index (n) with increasing capillary length reflect more fully developed shear flow and velocity profiles, as well as reduced entrance effects in longer dies. Shorter capillaries are more affected by entrance pressure drop and incomplete flow development, which can lead to overestimation of shear stress and consequently overestimate the K value. In contrast, the flow behavior index n remains relatively constant across different die lengths, suggesting that die length influences the magnitude of shear stress more than the shape of the flow curve. Comparison with previously reported values provides further insight into the rheological behavior of collagen dispersions. Štípek et al. [30] investigated a highly concentrated (7.7 wt%) water-based bovine collagen dispersion using slit capillary dies. They reported power law flow indices (n) ranging from 0.15 to 0.27 and consistency coefficients (K) from 644 to 2090 Pa·s^n. Similarly, Skočilas et al. [31] observed n values between 0.21 and 0.27 and K values between 860 and 2800 Pa·s^n for 6.6–8.0 wt% collagen dispersions. The close agreement in n values indicates that the present collagen dispersion exhibits comparable shear thinning behavior, despite its lower concentration.

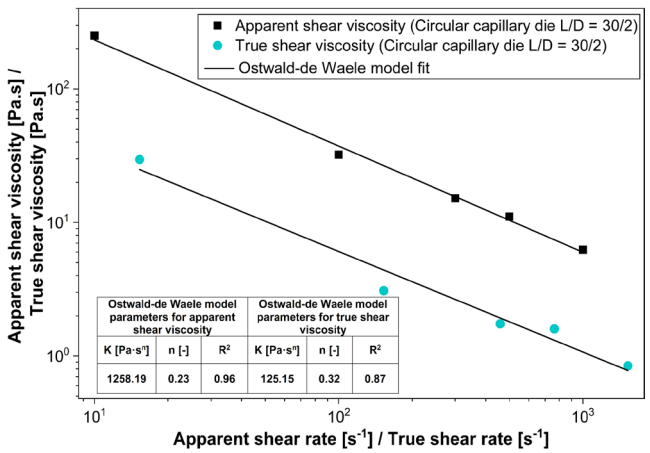

FIGURE 4 | Apparent and true shear viscosity versus apparent shear and true shear rate for collagen 3 wt% for capillary $L/D = 30/2$.

3.2 | Entrance Pressure Determination

Figure 5 shows Bagley plots for the collagen dispersion using circular capillary dies with L/D ratios of 5, 10, and 15 at different shear rates. A linear fit was applied to the experimental total pressure drop data. The extrapolation of these lines to $L/D = 0$ provided the entrance pressure drop for each shear rate by the intersection of the lines with the y-axis. The close alignment between the fitted lines and the experimental points indicates that the linear extrapolation is reliable for determining the entrance pressure drop. Figure 6 presents the entrance pressure drop obtained from both the Bagley correction and the orifice die method. The two methods agree closely across the examined shear rate range, indicating good consistency between the approaches. A deviation occurs at the lowest shear rate, where the orifice die yields lower entrance pressure value. For a low shear rate, the shear stress, even for a very short capillary, cannot be neglected. Table 3 summarizes the entrance pressure drop (ΔP_{Ent}) values, The relative error of the Bagley plots intercept, and relative error between Bagley and orifice die methods for a 3 wt% collagen dispersion. The relative errors of the Bagley plots intercept ranged from 0.80% to 5.94%. Comparison with the relative error between the Bagley correction and orifice die methods indicates that the uncertainty associated with the Bagley intercept is generally comparable to or lower than the error between the two approaches, supporting the reliability of the entrance pressure determination. The relative error is highest at lower shear rate but decreases rapidly with increasing shear rate. This trend

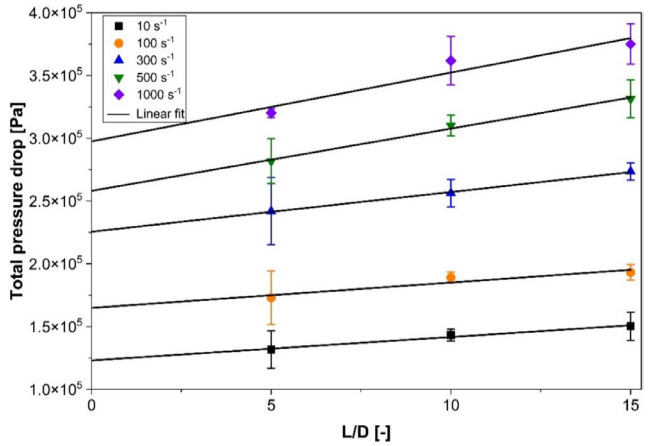

FIGURE 5 | Bagley plots at different shear rates for a 3 wt% collagen dispersion using three circular capillary dies with L/D ratios of 5, 10, and 15.

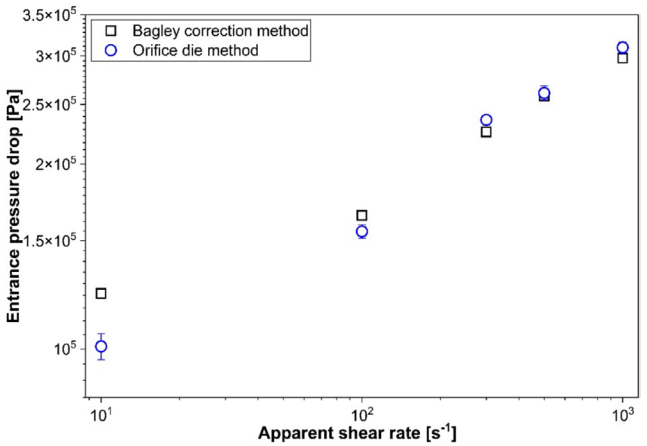

FIGURE 6 | Comparison of the entrance pressure drop obtained from the Bagley correction and orifice die method for a 3 wt% collagen dispersion over the investigated apparent shear rate.

TABLE 3 | Entrance pressure drop values obtained from the Bagley correction and the orifice die method for collagen 3 wt%.

Apparent shear rate (1/s)	ΔP_{Ent} (kPa) (Bagley)	Relative error of Bagley plot intercept (%)	ΔP_{Ent} (kPa) (Orifice die)	Relative error between methods (%)
10	123.05	2.28	100.94	17.97
100	164.85	4.59	155.34	5.77
300	225.55	0.80	235.99	4.63
500	258.13	1.77	261.01	1.12
1000	297.52	5.94	309.60	4.06

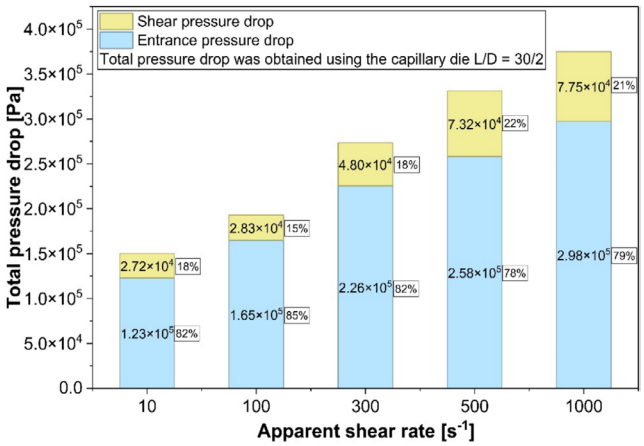

FIGURE 7 | Relative contributions of shear and entrance pressure drop to the total pressure drop as a function of apparent shear rate for a 3 wt% collagen dispersion (entrance pressure drop was determined using the Bagley correction method).

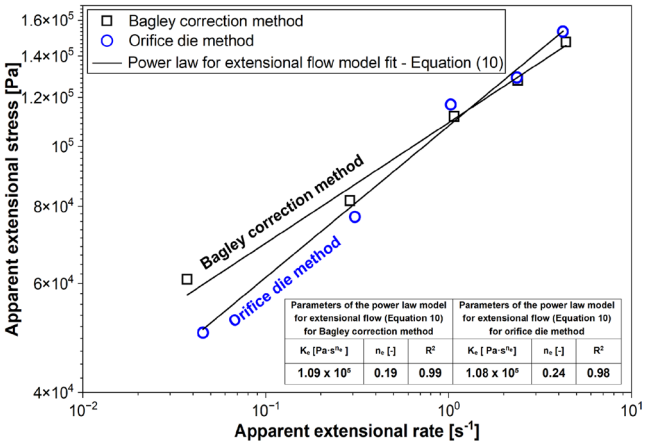

FIGURE 8 | Apparent extensional stress versus apparent extensional rate for collagen 3 wt%.

shows that the agreement between the methods improves considerably as the flow becomes more stable at higher deformation rates. When compared with measurements reported for polymer melts, the relative errors observed in this study are notably lower. Aho and Syrjala [24] reported relative errors of approximately 11%–19% for LDPE and 23%–53% for PS, where the orifice die provided entrance pressure drop values higher than those obtained by Bagley extrapolation. Sunder and Goettfert [20] found that the orifice die produced entrance pressures 10%–100% higher than those obtained by Bagley extrapolation for LDPE and PP. The results were attributed to the melt adhesion at the die exit region. In contrast, the collagen dispersion examined in this study shows good agreement between the two methods. This agreement indicates that both the Bagley and orifice die approaches provide reliable estimates of the entrance pressure drop. The good agreement also suggests that the selected L/D ratios (5, 10, and 15) were appropriate for accurate Bagley extrapolation.

Figure 7 shows the contribution of shear and entrance pressure drops to the total pressure drop at different apparent shear rates. The entrance pressure drop presented in this figure was determined using the Bagley correction method. The results show that the entrance pressure drop represents the dominant portion of the total pressure drop over the entire shear rate range. In contrast, the shear pressure drop represents a comparatively smaller fraction. These results indicate that the flow of collagen dispersion is primarily dominated by extensional deformation at the entrance.

3.3 | Extensional Flow Behavior

Figure 8 presents the apparent extensional stress as a function of the apparent extensional rate for the collagen dispersion. The data were obtained using both the Bagley correction and the orifice die method. The datasets are described by the power law model for extensional flow (Equation 10), and Table 4 presents the obtained parameters.

Figure 9 presents a comparison between the apparent extensional viscosity, apparent entrance viscosity (determined using both the Bagley correction and orifice die methods), and the apparent shear viscosity (measured with a circular capillary die, $L/D = 30/2$) as a function of the corresponding apparent extensional and shear rates.

The results show that the extensional viscosity remains higher than the shear viscosity across the entire extensional rate range. The significantly higher extensional viscosity compared with shear viscosity indicates that extensional deformation contributes significantly to flow resistance and should therefore be considered when describing the processing behavior of collagen dispersions in processes involving stretching or elongational flow, such as extrusion and contraction flows. This behavior exceeds several times the Trouton ratio, which predicts an extensional-to-shear viscosity ratio

TABLE 4 | Evolution of the power law model for extensional flow (Equation 10).

Method	K_e (Pa·s^{n_e})	Relative error of K_e (%)	n_e (–)	Relative error of n_e (%)	R^2
Bagley	1.09×10^5	1.46	0.19	5.69	0.99
Orifice die	1.08×10^5	2.56	0.24	8.45	0.98

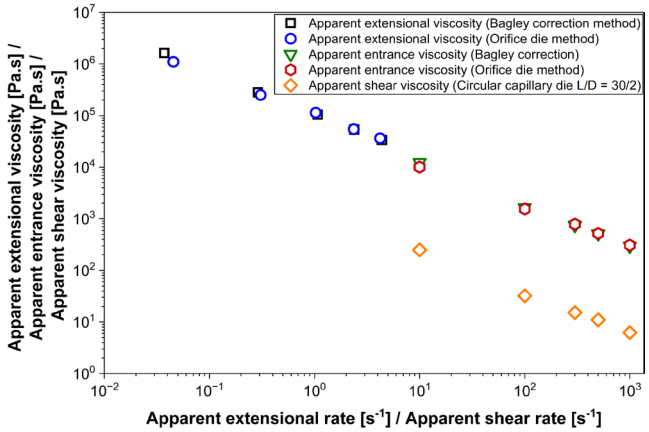

FIGURE 9 | Apparent extensional viscosity, apparent entrance viscosity, and apparent shear viscosity versus apparent extensional/shear rate for a 3 wt% collagen dispersion.

of three for Newtonian fluids [45]. In our study, the extensional viscosity of the 3 wt% collagen dispersion exceeded the shear viscosity by two to four orders of magnitude across the tested deformation rates, indicating a pronounced viscoelastic response. Similar deviations from the Trouton ratio have been reported in other food-based biopolymers [32, 43]. Núñez et al. [43] observed Trouton ratio ranging from 250 to 2200 in cereal-based pastes. Similarly, Lan et al. [32] reported that a collagen solution with a concentration of 0.23 wt% exhibited a Trouton ratio of 10. This highlights the dominant contribution of extensional flow resistance in collagen dispersion rheology. The figure indicates pronounced extensional thinning behavior of the collagen dispersion. This behavior can be attributed to molecular alignment and reduced intermolecular resistance under elongational flow. Similar extensional thinning behavior has been widely reported in viscoelastic food-based polymers such as breakfast cereal pastes [43], protein blends [46], xanthan gum solutions [47], oat suspensions [48], and wheat dough [49]. This emphasizes the characteristic nature of extensional thinning in many food biopolymer systems. On the other hand, the entrance viscosity is consistently higher than the shear viscosity. This indicates that the entry flow region contributes more significantly to the overall flow resistance than the shear flow within the capillary. The close agreement between the Bagley and orifice die methods further validates the entrance pressure drop approach and supports the validity of the extensional viscosity values calculated using the Cogswell analysis. Table 4 shows that the coefficients of fitting determination ($R^2 > 0.98$) and relatively low relative errors of the fitted parameters indicate that the power law model for extensional flow provides an excellent description of the measured behavior. The resulting model parameters yield extensional flow indices of $n_e = 0.19$ for the Bagley method and $n_e = 0.24$ for the orifice die. These values confirm the pronounced extension thinning behavior of the collagen dispersion. The corresponding consistency coefficients are also very similar in magnitude, demonstrating strong agreement between the two methods. These results indicate that both the Bagley correction and the orifice die method provide reliable estimates of the extensional flow characteristics of the collagen dispersion.

From a food processing perspective, these findings are directly relevant to applications like collagen extrusion (e.g., sausage casing production), where the material exhibits both shear and extensional deformation components. Accurate rheological modeling of such processes requires the inclusion of both components. Importantly, our measurements indicate that entrance pressure represents 78%–85% of the total pressure drop, suggesting that exclusion of extensional effects in process design could lead to major underestimation of required operational forces. Furthermore, our experimental results can provide valuable input for future development of constitutive models and computational simulations of collagen flows. Additionally, these data allow direct comparisons with other biopolymers to assess how the extensional resistance of other biopolymers compares to collagen.

3.4 | Oscillatory Strain Amplitude and Frequency Sweeps

Figure 10a shows the storage modulus (G′), loss modulus (G″), and the relative intensity of the harmonic ratio I_3/I_1 of the 3 wt% native collagen dispersion as a function of oscillatory strain at a constant frequency of $\omega = 1$ Hz. At low strain amplitudes, both moduli remain nearly constant, indicating that the material is within the linear viscoelastic regime (LVE). In this regime, G′ is significantly higher than G″, demonstrating a solid-like response. In the study of Štípek et al. [39], the viscoelastic properties of water-based native bovine collagen gels were investigated over a wide range of collagen mass fractions from 1.5 to 7.6 wt%. The authors reported that, in the linear viscoelastic regime, the storage modulus was higher than the loss modulus, indicating solid-like viscoelastic behavior. Furthermore, both storage and loss moduli increased significantly with increasing collagen concentration. Similarly, Šupová et al. [28] investigated the viscoelastic properties of water-based native bovine collagen gels with fraction of 5 wt%. Their oscillatory rheology measurements showed that collagen gels exhibit dominant elastic behavior and viscoelastic solid-like properties in the linear viscoelastic regime. In addition, they reported that the rheological properties of collagen gels are strongly influenced by the structural organization and orientation of collagen fibrils.

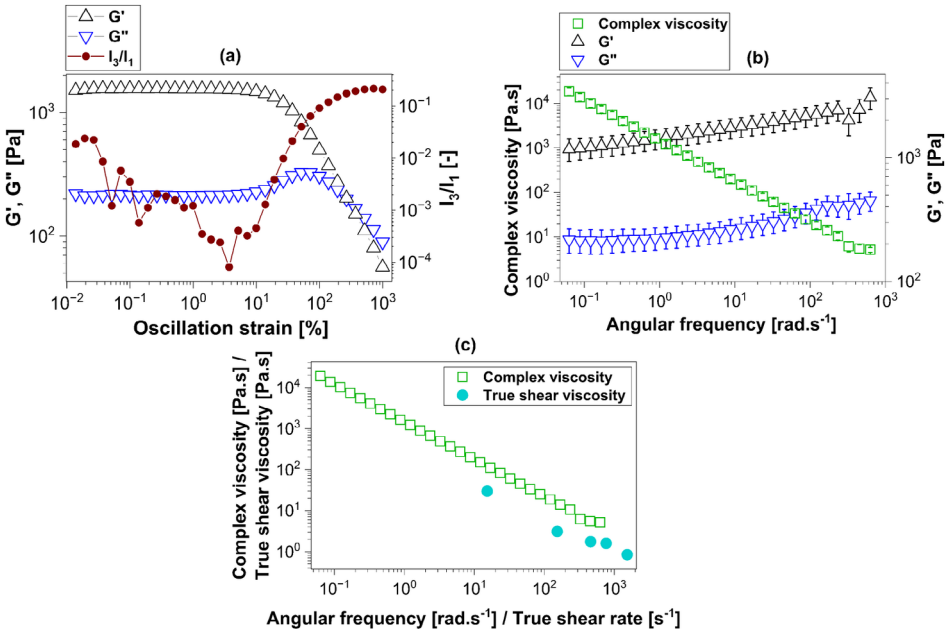

FIGURE 10 | Oscillatory rheological behavior of 3 wt% collagen dispersion showing (a) strain amplitude sweep, (b) frequency sweep, and (c) comparison of absolute value of the complex viscosity and true shear viscosity.

The nonlinear viscoelastic response was quantified using the harmonic ratio I_3/I_1. Figure 10a shows that at low strain amplitudes, $I_3/I_1 \cong 1.22 \times 10^{-3}$ at strain amplitude of $\gamma_0 \cong 1\%$ and has value of $I_3/I_1 \cong 1.28 \times 10^{-3}$ at $\gamma_0 \cong 13\%$, with fluctuations observed in the range of $\gamma_0 \cong 1\%$–13%. Beyond this range, I_3/I_1 ratio increases, reaching value of $I_3/I_1 \cong 3.88 \times 10^{-3}$ at $\gamma_0 \cong 19\%$ and continuing to rise significantly at higher strain amplitudes. This behavior indicates the progressive development of nonlinear viscoelasticity, which can be associated with structural rearrangement and eventual breakdown of the collagen network. The results also show a weak strain overshoot behavior in the loss modulus in the nonlinear viscoelastic regime. This phenomenon has been widely reported in food-based viscoelastic materials such as protein dispersions [50], starch paste [51], gelatin [52], and xanthan gum solution [53]. Hyun et al. [53] explained that the increase in the loss modulus prior to the overshoot for xanthan gum solution is attributed to structural rearrangement that enhances the resistance to applied deformation, while the decrease in the loss modulus at higher strain amplitudes is attributed to progressive structural breakdown. This behavior is characteristic of structured viscoelastic materials under nonlinear deformation and transition from solid-like to liquid-like behavior. A similar weak strain overshoot behavior has also been reported for collagen gels by Štípek et al. [39]. In contrast, the amplitude sweep results reported by Šupová et al. [28] for collagen gels did not show a pronounced loss modulus overshoot. This difference could be attributed to differences in collagen structure, network organization, the range of strain amplitudes used in the amplitude sweep tests, and sample preparation conditions.

Figure 10b shows the frequency sweep results measured within the linear viscoelastic regime at a fixed strain amplitude of $\gamma_0 = 1.0\%$. No crossover point between the storage and loss modulus was observed over the investigated frequency range, indicating the presence of an entangled fibrillar network in the collagen dispersion. The complex viscosity decreases with increasing frequency, indicating shear-thinning behavior and progressive alignment and partial disruption of the collagen network at higher deformation rates. Such behavior is typical for structured soft materials such as gels [54–56].

Figure 10c compares the absolute value of the complex viscosity obtained from oscillatory measurements with the true shear viscosity obtained from capillary rheometer to investigate the applicability of the Cox–Merz rule [57]. According to this rule, the complex viscosity measured in oscillatory shear at a given angular frequency ω (rad.s^{-1}) is approximately equal to the steady shear viscosity measured at the corresponding shear rate $\dot{\gamma}$ (s^{-1}), assuming $\omega = \dot{\gamma}$. Figure 10c shows that for the collagen dispersion; the shear viscosity is consistently lower than the complex viscosity across the examined deformation range. This deviation indicates that the Cox–Merz rule is not applicable to the present collagen system. Similar deviations have been reported for various biopolymer and hydrogel systems [54–56]. The deviation from the Cox–Merz rule observed in the present study can be attributed to the structured nature of collagen dispersions. Structured soft materials such as gels often do not follow the Cox–Merz rule because the measured viscosity depends strongly on the applied flow profile and the degree of structural disruption during deformation [55, 56]. Oscillatory measurements performed in the linear viscoelastic regime preserve the network structure and therefore result in higher apparent viscosities, whereas steady shear measurements may induce structural rearrangement, or partial breakdown of the network, leading to lower viscosity values [55, 56]. The deviation from the Cox–Merz rule therefore indicates that the collagen dispersion behaves as a structured, shear-sensitive network rather than a simple polymer solution.

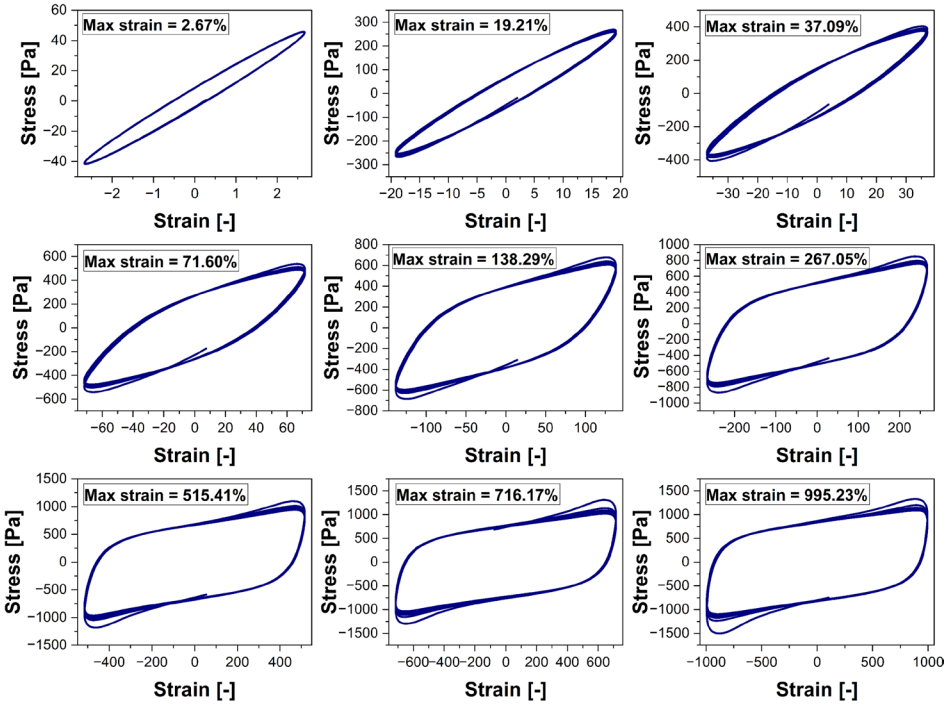

FIGURE 11 | Stress–strain Lissajous–Bowditch curves obtained from large amplitude oscillatory shear (LAOS) measurements of 3 wt% collagen dispersion at different strain amplitudes ranging from 2.7% to 995% at a constant frequency of 1 Hz.

3.5 | Large Amplitude Oscillatory Shear (LAOS)

Figure 11 presents the stress–strain Lissajous–Bowditch curves obtained from large amplitude oscillatory shear (LAOS) measurements for the 3 wt% collagen dispersion at different strain amplitudes ranging from approximately 2.7% to 995%. At low strain amplitudes (approximately 2.7%), the Lissajous curves exhibit an elliptical shape, indicating near-linear viscoelastic behavior where the stress response is proportional to the applied strain. As the strain amplitude increases (approximately 3%–100%), the curves progressively deviate from an elliptical shape and become distorted, indicating nonlinear viscoelastic behavior and increased energy dissipation due to structural rearrangement of the collagen network. At higher strain amplitudes (approximately > 100%), the curves become more rectangular, indicating structural breakdown and viscous flow behavior of the collagen network. The evolution of the Lissajous curves from elliptical to distorted and rectangular shapes indicates a gradual transition from linear viscoelastic behavior to nonlinear viscoelastic behavior at increasing strain amplitudes. Similar nonlinear viscoelastic behavior using Lissajous curves evolution have been reported for food-based materials such as 6 wt% collagen dispersion [39], concentrated protein solutions [58], and rice starch gels [59].

To further quantify the nonlinear viscoelastic behavior observed in the LAOS measurements, Fourier transform rheology (commonly known as FT-rheology) was applied. FT-rheology provides a powerful tool for analyzing nonlinear viscoelastic behavior by decomposing the stress response into harmonic contributions [60–62]. In the linear viscoelastic regime, the stress signal is dominated by the first harmonic, whereas the appearance of higher odd harmonics indicates the transition from linear to nonlinear viscoelastic behavior [60–62]. In particular, the harmonic intensity ratios I_n/I_1, such as I_3/I_1, provide a quantitative measure of nonlinearity which may not be provided from Lissajous–Bowditch analysis. Figure 12 presents the time-domain stress signals and the corresponding frequency-domain spectra at different strain amplitudes. The nonlinear viscoelastic response was quantified using the harmonic ratio I_n/I_1. FT-rheology has been widely applied to various soft and food-based materials, including xanthan gum [63, 64], hyaluronic acid [63], egg white protein foams [64], and peanut butter [65].

The FT spectra in Figure 12 show that the contribution of higher harmonics increases with increasing deformation, confirming the transition from linear to nonlinear response. At moderate strain ($\gamma_0 \cong 37\%$), the third harmonic contribution remains relatively small ($I_3/I_1 \cong 0.02$), indicating weak nonlinearity. A small contribution of the fifth harmonic ($I_5/I_1 \cong 0.002$) is also observed. With increasing strain amplitude ($\gamma_0 \cong 138\%$), the contribution of higher harmonics increases (e.g., $I_3/I_1 \cong 0.11$), reflecting the onset of nonlinear behavior. At large strain amplitudes ($\gamma_0 \cong 995\%$), a significant increase in harmonic intensity is observed (e.g., $I_3/I_1 \cong 0.21$), along with the appearance of higher-order harmonics (e.g., I_9/I_1, I_{11}/I_1), indicating strong nonlinear viscoelasticity. The progressive increase in higher harmonic intensities indicates a transition from linear viscoelastic behavior to a strongly nonlinear regime. This behavior can be attributed to structural rearrangements within the collagen network, including alignment, stretching, and partial breakdown of fibrillar structures under large deformation. These findings are consistent with the Lissajous–Bowditch analysis, where deviations from elliptical shapes and the development of distorted stress–strain loops were observed at higher strain amplitudes. The present FT-rheology results can be used to distinguish between different collagen dispersions exhibiting similar SAOS behavior,

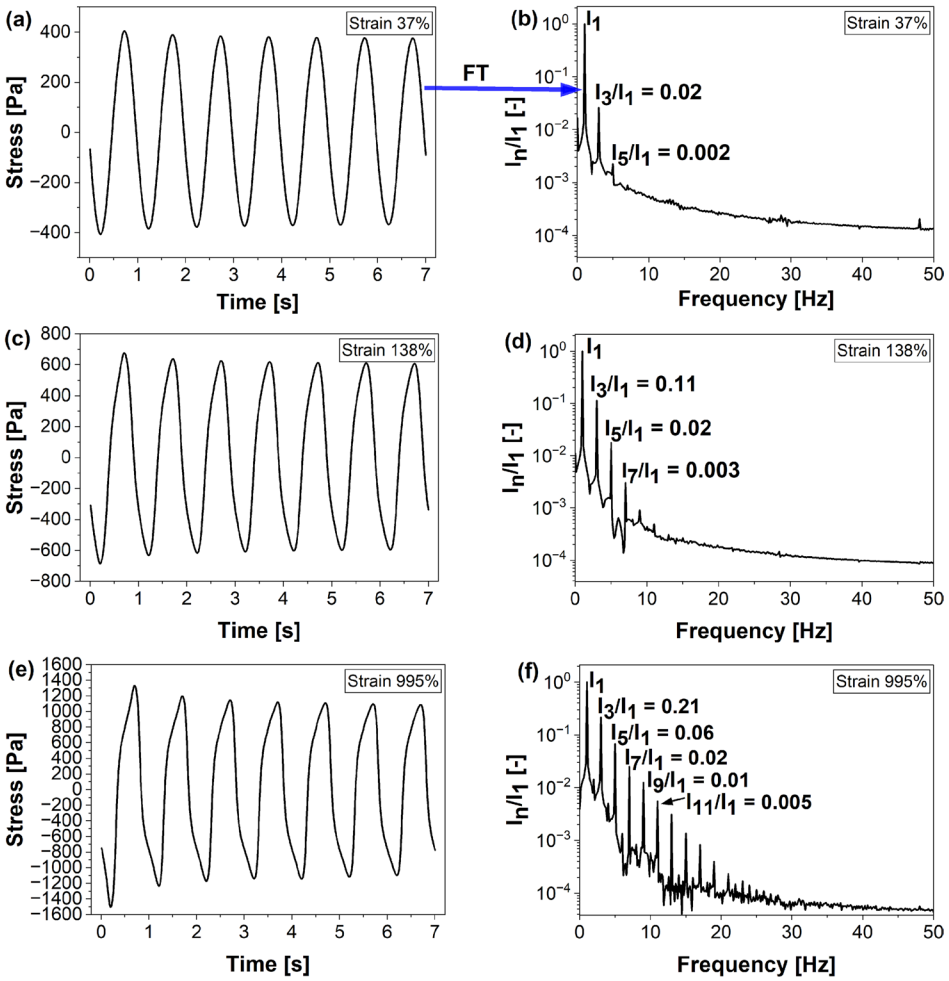

FIGURE 12 | Time-domain stress responses of the collagen dispersion at different strain amplitudes (a), (c), and (e) and their corresponding FT spectra in the frequency domain (b), (d), and (f). The intensity of the higher harmonics (I_n/I_1) is presented on a logarithmic y-scale.

as variations in higher harmonic intensities can provide a sensitive indicator of differences in collagen structure and nonlinear deformation response. On the other hand, it can provide a quantitative basis for predicting the nonlinear response of collagen dispersions under processing-relevant deformation conditions.

4 | Conclusions

This study presented a comprehensive rheological investigation of a 3 wt% native bovine collagen dispersion. Entrance pressure drop was determined using both Bagley correction and a modified orifice die, and extensional viscosity was estimated using Cogswell's analysis. Capillary rheometer results showed strong shear-thinning and extensional-thinning behavior of collagen, with extensional viscosity significantly exceeding shear viscosity over the entire deformation rate range. The close agreement between Bagley extrapolation and the orifice die method confirmed the reliability of the entrance pressure determination and validated the fabricated orifice die for direct entrance pressure measurements. The oscillatory shear results showed that the collagen dispersion exhibits solid-like behavior in the linear viscoelastic regime. LAOS analysis indicated progressive structural breakdown and nonlinear viscoelastic behavior with increasing strain amplitude. FT-rheology provided a quantitative characterization of the nonlinear viscoelastic response through harmonic intensity ratios. The progressive increase of higher harmonics with strain amplitude confirmed the transition from linear to nonlinear behavior of collagen. This work provides new insights into the flow behavior of water-based native collagen systems under shear and extensional flow conditions relevant to food and biopolymer processing. The combined rheological analysis provides a quantitative description of collagen behavior under shear, extensional, and oscillatory deformation. By linking measured viscosities and harmonic intensity ratios to deformation conditions, the results enable prediction of flow behavior under processing-relevant conditions. These findings provide quantitative input for modeling, design, and optimization of processing operations involving collagen dispersions, particularly extrusion processes. Furthermore, the methodology applied in this study has potential for integration into inline measurement systems, enabling real-time process monitoring, quality control, and improved process efficiency. While this study provides a comprehensive rheological characterization of a low-concentration collagen dispersion relevant to industrial processing, future work could investigate the influence of concentration, temperature, shear-induced molecular weight degradation, and structural organization on the rheological behavior of collagen dispersions under different processing conditions.

Author Contributions

Fadi Alzarzouri: writing – original draft, writing – review and editing, methodology, investigation, data curation, formal analysis, visualization, conceptualization. **Xiaohe Xu:** writing – review and editing, methodology, investigation, conceptualization. **Manfred Wilhelm:** supervision, writing – review and editing. **Jan Skočilas:** supervision, writing – review and editing.

Acknowledgments

The authors thank Dr. Michael Pollard for the language revision of the English manuscript. Thanks are extended to the Institute of Chemical Technology and Polymer Chemistry, Karlsruhe Institute of Technology, for providing laboratory facilities and technical support during this research. Open access publishing facilitated by Ceske vysoke uceni technicke v Praze, as part of the Wiley - CzechELib agreement.

Conflicts of Interest

The authors declare no conflicts of interest.

Data Availability Statement

Data will be made available on request.

References

1. E. Dalle Fratte, D. R. D'hooge, M. Eeckhout, and L. Cardon, "Principles and Guidelines for In-Line Viscometry in Cereal Extrusion," *Polymers* 14, no. 12 (2022): 2316, https://doi.org/10.3390/polym14122316.

2. V. Evageliou, "Shear and Extensional Rheology of Selected Polysaccharides," *International Journal of Food Science and Technology* 55, no. 5 (2020): 1853–1861, https://doi.org/10.1111/ijfs.14545.

3. F. J. Galindo-Rosales, M. A. Alves, and M. S. Oliveira, "Microdevices for Extensional Rheometry of Low Viscosity Elastic Liquids: A Review," *Microfluidics and Nanofluidics* 14, no. 1 (2013): 1–19, https://doi.org/10.1007/s10404-012-1028-1.

4. M. Padmanabhan, "Measurement of Extensional Viscosity of Viscoelastic Liquid Foods," *Journal of Food Engineering* 25, no. 3 (1995): 311–327, https://doi.org/10.1016/0260-8774(94)00016-3.

5. G. Della Valle, M. Dufour, F. Hugon, H. Chiron, L. Saulnier, and K. Kansou, "Rheology of Wheat Flour Dough at Mixing," *Current Opinion in Food Science* 47 (2022): 100873, https://doi.org/10.1016/j.cofs.2022.100873.

6. A. Parhi, A. Verma, P. K. Nair, and P. Sharma, "Invited Review: Manufacture and Quality Control of Mozzarella Cheese—Scientific and Technological Advances," *Journal of Dairy Science* 108, no. 11 (2025): 11802–11823, https://doi.org/10.3168/jds.2024-26225.

7. M. L. Sentmanat, "Miniature Universal Testing Platform: From Extensional Melt Rheology to Solid-State Deformation Behavior," *Rheologica Acta* 43, no. 6 (2004): 657–669, https://doi.org/10.1007/s00397-004-0405-4.

8. P. Hodder and A. Franck, "A New Tool for Measuring Extensional Viscosity," *Annual Transactions of the Nordic Rheology Society* 13 (2005): 227–232.

9. M. Khabazian Esfahani, C. K. Georgantopoulos, I. F. Naue, J. Sunder, and M. Wilhelm, "A New Slit-Radial Die for Simultaneously Measuring Steady State Shear Viscosity and First Normal Stress Difference of Viscoelastic Liquids via Capillary Rheometry," *Journal of Applied Polymer Science* 139, no. 18 (2022): 52094, https://doi.org/10.1002/app.52094.

10. V. Hirschberg, S. Lyu, M. G. Schußmann, M. Wilhelm, and M. H. Wagner, "Modeling Elongational Viscosity of Polystyrene Pom-Pom/Linear and Pom-Pom/Star Blends," *Rheologica Acta* 62, no. 9 (2023): 433–445, https://doi.org/10.1007/s00397-023-01411-1.

11. V. Hirschberg, L. Faust, M. Abbasi, Q. Huang, M. Wilhelm, and M. H. Wagner, "Hyperstretching in Elongational Flow of Densely Grafted Comb and Branch-on-Branch Model Polystyrenes," *Journal of Rheology* 68, no. 2 (2024): 229–246, https://doi.org/10.1122/8.0000781.

12. G. H. McKinley and T. Sridhar, "Filament-Stretching Rheometry of Complex Fluids," *Annual Review of Fluid Mechanics* 34, no. 1 (2002): 375–415, https://doi.org/10.1146/annurev.fluid.34.083001.125207.

13. K. Riazi, M. Abbasi, C. O. Klein, I. F. Naue, and M. Wilhelm, "Quantifying Separation Energy With a Modified Capillary Break-Up Extensional Rheometer to Study Polymer Solutions," *Soft Matter* 19, no. 2 (2021): 199–212, https://doi.org/10.1080/1539445X.2020.1792929.

14. C. O. Klein, I. F. Naue, J. Nijman, and M. Wilhelm, "Addition of Force Measurement Capability to a Commercially Available Extensional Rheometer," *Soft Matter* 7, no. 4 (2009): 242–257, https://doi.org/10.1080/15394450903444603.

15. M. Padmanabhan and M. Bhattacharya, "Planar Extensional Viscosity of Corn Meal Dough," *Journal of Food Engineering* 18, no. 4 (1993): 389–411, https://doi.org/10.1016/0260-8774(93)90054-N.

16. M. Padmanabhan and C. W. Macosko, "Extensional Viscosity From Entrance Pressure Drop Measurements," *Rheologica Acta* 36, no. 2 (1997): 144–151, https://doi.org/10.1007/BF00366820.

17. F. N. Cogswell, "Converging Flow of Polymer Melts in Extrusion Dies," *Polymer Engineering and Science* 12, no. 1 (1972): 64–73, https://doi.org/10.1002/pen.760120111.

18. F. N. Cogswell, "Converging Flow and Stretching Flow: A Compilation," *Journal of Non-Newtonian Fluid Mechanics* 4, no. 1–2 (1978): 23–38, https://doi.org/10.1016/0377-0257(78)85004-6.

19. E. B. Bagley, "End Corrections in the Capillary Flow of Polyethylene," *Journal of Applied Physics* 28, no. 5 (1957): 624–627, https://doi.org/10.1063/1.1722814.

20. J. Sunder and A. Goettfert, "Extensional Flow Properties From Entrance Pressure Measurements Using Zero Length Die Versus Bagley Correction," in *ANTEC 2001 Conference Proceedings* (Society of Plastics Engineers (SPE), 2001), 6.

21. A. L. Kelly, P. D. Crates, T. W. Dobbie, and D. J. Fleming, "On Line Rheometry: Shear and Extensional Flows," *Plastics, Rubber and Composites Processing and Applications* 25, no. 7 (1996): 313–318.

22. S. Kim and J. M. Dealy, "Design of an Orifice Die to Measure Entrance Pressure Drop," *Journal of Rheology* 45, no. 6 (2001): 1413–1419, https://doi.org/10.1122/1.1410374.

23. M. Zatloukal and J. Musil, "Analysis of Entrance Pressure Drop Techniques for Extensional Viscosity Determination," *Polymer Testing* 28, no. 8 (2009): 843–853, https://doi.org/10.1016/j.polymertesting.2009.07.007.

24. J. Aho and S. Syrjala, "Determination of the Entrance Pressure Drop in Capillary Rheometry Using Bagley Correction and Zero-Length Capillary," *Annual Transactions of the Nordic Rheology Society* 14 (2006): 143.

25. V. de Melo Oliveira, C. R. D. Assis, B. D. A. M. Costa, et al., "Physical, Biochemical, Densitometric and Spectroscopic Techniques for Characterization of Collagen From Alternative Sources," *Journal of Molecular Structure* 1224 (2021): 129023, https://doi.org/10.1016/j.molstruc.2020.129023.

26. P. Suurs and S. Barbut, "Collagen Use for Co-Extruded Sausage Casings: A Review," *Trends in Food Science and Technology* 102 (2020): 91–101, https://doi.org/10.1016/j.tifs.2020.06.011.

27. C. Tang, K. Zhou, Y. Zhu, et al., "Collagen and Its Derivatives: From Structure and Properties to Their Applications in Food Industry," *Food Hydrocolloids* 131 (2022): 107748, https://doi.org/10.1016/j.foodhyd.2022.107748.

28. M. Šupová, T. Suchý, H. Chlup, et al., "Evaluation of Two Collagen Gels Used for Sausage Casing Extrusion," *Journal of Food Engineering* 343 (2023): 111387, https://doi.org/10.1016/j.jfoodeng.2022.111387.

29. J. Skočilas, R. Žitný, J. Štancl, et al., "Flow of Bovine Collagen in Rectangular Slit," *AIP Conference Proceedings* 1843 (2017): 50003, https://doi.org/10.1063/1.4982995.

30. J. Štípek, J. Skočilas, J. Štancl, and R. Žitný, "Extrusion Rheometry of Collagen Dough," *Czech Journal of Food Sciences* 39, no. 5 (2021): 384–392, https://doi.org/10.17221/265/2020-CJFS.

31. J. Skočilas, R. Žitný, J. Štancl, M. Dostál, A. Landfeld, and M. Houška, "Rheological Properties of Collagen Matter Predicted Using an Extrusion Rheometer," *Journal of Texture Studies* 47, no. 6 (2016): 514–522, https://doi.org/10.1111/jtxs.12194.

32. X. Lan, A. Adesida, and Y. Boluk, "Rheological and Viscoelastic Properties of Collagens and Their Role in Bioprinting by Micro-Extrusion," *Biomedical Materials* 17, no. 6 (2022): 62005, https://doi.org/10.1088/1748-605X/ac9b06.

33. H. Yang, L. Duan, Q. Li, Z. Tian, and G. Li, "Experimental and Modeling Investigation on the Rheological Behavior of Collagen Solution as a Function of Acetic Acid Concentration," *Journal of the Mechanical Behavior of Biomedical Materials* 77 (2018): 125–134, https://doi.org/10.1016/j.jmbbm.2017.09.003.

34. S. Motte and L. J. Kaufman, "Strain Stiffening in Collagen I Networks," *Biopolymers* 99, no. 1 (2013): 35–46, https://doi.org/10.1002/bip.22133.

35. F. Gobeaux, E. Belamie, G. Mosser, P. Davidson, and S. Asnacios, "Power Law Rheology and Strain-Induced Yielding in Acidic Solutions of Type I Collagen," *Soft Matter* 6, no. 16 (2010): 3769–3777, https://doi.org/10.1039/B922151D.

36. N. Saeidi, E. A. Sander, and J. W. Ruberti, "Dynamic Shear-Influenced Collagen Self-Assembly," *Biomaterials* 30, no. 34 (2009): 6581–6592, https://doi.org/10.1016/j.biomaterials.2009.07.070.

37. N. A. Kurniawan, L. H. Wong, and R. Rajagopalan, "Early Stiffening and Softening of Collagen: Interplay of Deformation Mechanisms in Biopolymer Networks," *Biomacromolecules* 13, no. 3 (2012): 691–698, https://doi.org/10.1021/bm2015812.

38. T. Zheng, P. Tang, L. Shen, H. Bu, and G. Li, "Rheological Behavior of Collagen/Chitosan Blended Solutions," *Journal of Applied Polymer Science* 138, no. 34 (2021): 50840, https://doi.org/10.1002/app.50840.

39. J. Štípek, H. Rohm, T. Suchý, et al., "Characterization of Structural Properties and Non-Linear Rheological Behavior of Collagen Over a Wide Range of Mass Fractions Under Laos," *Polymer Engineering and Science* 65, no. 6 (2025): 3018–3028, https://doi.org/10.1002/pen.27195.

40. M. Zatloukal, J. Vlček, C. Tzoganakis, and P. Sáha, "Improvement in Techniques for Determination of Extensional Rheological Data From Entrance Flows," *Journal of Non-Newtonian Fluid Mechanics* 107, no. 1–3 (2002): 13–37, https://doi.org/10.1016/S0377-0257(02)00111-8.

41. Z. Zhang and S. G. Hatzikiriakos, "Entry Pressure Correlations in Capillary Flow," *Physics of Fluids* 32, no. 7 (2020): 073106-1–073106-10, https://doi.org/10.1063/5.0017922.

42. D. M. Binding, "An Approximate Analysis for Contraction and Converging Flows," *Journal of Non-Newtonian Fluid Mechanics* 27, no. 2 (1988): 173–189, https://doi.org/10.1016/0377-0257(88)85012-2.

43. M. Núñez, G. Della Valle, and A. J. Sandoval, "Shear and Elongational Viscosities of a Complex Starchy Formulation for Extrusion Cooking," *Food Research International* 43, no. 8 (2010): 2093–2100, https://doi.org/10.1016/j.foodres.2010.07.006.

44. D. T. Uchida, D. S. T. Ogassawara, and M. L. Bruschi, "Binary Polymeric System Based on Fish Collagen and Poloxamer 407: Mechanical and Rheological Analysis for Pharmaceutical and Biomedical Applications," *ACS Omega* 10 (2025): 53927–53958, https://doi.org/10.1021/acsomega.5c04058.

45. C. J. Petrie, "Extensional Viscosity: A Critical Discussion," *Journal of Non-Newtonian Fluid Mechanics* 137, no. 1–3 (2006): 15–23, https://doi.org/10.1016/j.jnnfm.2006.01.011.

46. T. Purcell, G. Delaplace, A. Riaublanc, M. Demême, A. Derensy, and G. Della Valle, "A General Viscosity Model for High Moisture Extrudates of Pea Protein Isolates/Gluten Blend," *Physics of Fluids* 37, no. 3 (2025): 033120-1–033120-10, https://doi.org/10.1063/5.0256835.

47. J. E. Martín-Alfonso, A. A. Cuadri, M. Berta, and M. Stading, "Relation Between Concentration and Shear-Extensional Rheology Properties of Xanthan and Guar Gum Solutions," *Carbohydrate Polymers* 181 (2018): 63–70, https://doi.org/10.1016/j.carbpol.2017.10.057.

48. L. Malafronte, S. Yilmaz-Turan, L. Dahl, F. Vilaplana, and P. Lopez-Sanchez, "Shear and Extensional Rheological Properties of Whole Grain Rye and Oat Aqueous Suspensions," *Food Hydrocolloids* 137 (2023): 108319, https://doi.org/10.1016/j.foodhyd.2022.108319.

49. E. Y. Arabo, "Shear and Extensional Viscosities of Hard Wheat Flour Dough Using a Capillary Rheometer," *Journal of Food Engineering* 103, no. 3 (2011): 294–298, https://doi.org/10.1016/j.jfoodeng.2010.10.027.

50. R. G. M. Van der Sman, P. Chakraborty, N. P. Hua, and N. Kollmann, "Scaling Relations in Rheology of Proteins Present in Meat Analogs," *Food Hydrocolloids* 135 (2023): 108195, https://doi.org/10.1016/j.foodhyd.2022.108195.

51. P. Boonkor, L. M. C. Sagis, and N. Lumdubwong, "Pasting and Rheological Properties of Starch Paste/Gels in a Sugar-Acid System," *Foods* 11, no. 24 (2022): 4060, https://doi.org/10.3390/foods11244060.

52. M. Rezaee, F. Ait Aider-Kaci, and M. Aider, "Effects of Hydrocolloids on Physicochemical and Rheological Properties of Pickering Emulsions Stabilized by Canola Protein Microgel," *ACS Food Science & Technology* 2, no. 10 (2022): 1681–1690, https://doi.org/10.1021/acsfoodscitech.2c00264.

53. K. Hyun, S. H. Kim, K. H. Ahn, and S. J. Lee, "Large Amplitude Oscillatory Shear as a Way to Classify Complex Fluids," *Journal of Non-Newtonian Fluid Mechanics* 107, no. 1–3 (2002): 51–65, https://doi.org/10.1016/S0377-0257(02)00141-6.

54. R. A. Mohamed Yunus and D. Parisi, "Scaling Laws in Polysaccharide Rheology: Comparative Analysis of Water and Ionic Liquid Systems," *Biomacromolecules* 25, no. 10 (2024): 6883–6898, https://doi.org/10.1021/acs.biomac.4c01125.

55. P. Bertsch, M. Diba, D. J. Mooney, and S. C. Leeuwenburgh, "Self-Healing Injectable Hydrogels for Tissue Regeneration," *Chemical Reviews* 123, no. 2 (2022): 834–873, https://doi.org/10.1021/acs.chemrev.2c00179.

56. M. Bercea, "Rheology as a Tool for Fine-Tuning the Properties of Printable Bioinspired Gels," *Molecules* 28, no. 6 (2023): 2766, https://doi.org/10.3390/molecules28062766.

57. W. P. Cox and E. H. Merz, "Correlation of Dynamic and Steady Flow Viscosities," *Journal of Polymer Science* 28, no. 118 (1958): 619–622, https://doi.org/10.1002/pol.1958.1202811812.

58. F. K. G. Schreuders, L. M. C. Sagis, I. Bodnár, P. Erni, R. M. Boom, and A. J. Van der Goot, "Small and Large Oscillatory Shear Properties of Concentrated Proteins," *Food Hydrocolloids* 110 (2021): 106172, https://doi.org/10.1016/j.foodhyd.2020.106172.

59. S. Precha-Atsawanan, D. Uttapap, and L. M. C. Sagis, "Linear and Nonlinear Rheological Behavior of Native and Debranched Waxy Rice Starch Gels," *Food Hydrocolloids* 85 (2018): 1–9, https://doi.org/10.1016/j.foodhyd.2018.06.050.

60. M. Wilhelm, D. Maring, and H. W. Spiess, "Fourier-Transform Rheology," *Rheologica Acta* 37, no. 4 (1998): 399–405, https://doi.org/10.1007/s003970050126.

61. M. Wilhelm, "Fourier-Transform Rheology," *Macromolecular Materials and Engineering* 287, no. 2 (2002): 83–105, https://doi.org/10.1002/1439-2054(20020201)287:2%3C83::AID-MAME83%3E3.0.CO;2-B.

62. K. Hyun, M. Wilhelm, C. O. Klein, et al., "A Review of Nonlinear Oscillatory Shear Tests: Analysis and Application of LAOS," *Progress in Polymer Science* 36, no. 12 (2011): 1697–1753, https://doi.org/10.1016/j.progpolymsci.2011.02.002.

63. K. Hyun, J. G. Nam, M. Wilhelm, K. H. Ahn, and S. J. Lee, "Nonlinear Response of Complex Fluids Under Laos Flow," *Korea-Australia Rheology Journal* 15, no. 2 (2003): 97–105.

64. P. Ptaszek, "Large Amplitude Oscillatory Shear Behavior of Egg White Foams With Apple Pectins and Xanthan Gum," *Food Research International* 62 (2014): 299–307, https://doi.org/10.1016/j.foodres.2014.03.002.

65. G. P. Citerne, P. J. Carreau, and M. Moan, "Rheological Properties of Peanut Butter," *Rheologica Acta* 40, no. 1 (2001): 86–96, https://doi.org/10.1007/s003970000120.